PROCEEDINGS, 47th Workshop on Geothermal Reservoir Engineering
Stanford University, Stanford, California, February 7-9, 2022
SGP-TR-223

An Experimental Method for Fast Evaluating the Function of Thermoelectric Generators

Ting Zhao[1,2], Kewen Li [1,2,*], Yuhao Zhu[1,2], Lin Jia[1,2], Xiaoyong Hou[3], Shuai Wang[3], and Mohammed Kaita[1,2]

[1]School of energy resources, China University of Geosciences (Beijing), 29 Xueyuan Road, 100083 Beijing, China

[2]Key laboratory of marine reservoir evolution and hydrocarbon enrichment mechanism, Ministry of Education

[3]Yangquan Coal Industry Group Co., Ltd.

[*]Corresponding Author: likewen@cugb.edu.cn

Keywords: Thermoelectric generators, Single pair PN legs, Experimental apparatus, Power generation, Fast evaluation of TEG

ABSTRACT

Thermoelectric generators (TEG) are widely used in many industries. The voltage and output power of TEG chips are critical indicators to evaluate the performance of TEGs. The conventional method is to directly test the output voltage and power of the whole TEG chip that contains 127 pairs of PN (P- and N-type) legs (127-PN-TEG). However, the assembling of these PN legs is very time-consuming. In order to reduce experimental time and the consumption of TEG materials, we proposed an experimental method. We developed the test apparatus for the rapid evaluation of TEG performance using a TEG chip with a single pair of PN legs (1-PN-TEG). We made several 1-PN-TEGs and 127-PN-TEGs using the same thermoelectric material (bismuth telluride). We then measured the voltage and the power of these 1-PN-TEGs and 127-PN-TEGs, respectively. The experimental results were compared and analyzed. The comparison showed that the voltage of 127-PN-TEG is equal to the voltage of 1-PN-TEG times 127, which implies that we could use the test data of 1-PN-TEG to evaluate the performance of 127-PN-TEG. Using the experimental device developed in this paper, we also studied the effects of the PN leg area (cross-sectional area of PN legs) and the pressure applied over the TEGs on the output power of 1-PN-TEG. The experimental results showed that the power per unit area decreases with an increase in the 1-PN-TEG's PN leg area when the temperature difference between the hot and cold sides was constant. Under a specific temperature difference conditions, the open-circuit voltage and the output power will increase with the pressure applied on the TEG chips.

1. INTRODUCTION

TEG technology can directly transform thermal energy into electricity through the Seebeck effect （Antonino et al., 2018）. It is an environmental-friendly and energy-saving technology （Jaziri et al., 2019; Wang et al., 2012）.TEG has been used in many fields such as waste heat recovery（Araiz et al., 2019; Crane et al., 2009）, solar cooling system no（Al-Nimr, et al., 2020; Li et al., 2015）, hybrid photovoltaic system （Shittu et al., 2019）, solar power generation （ Venkateshwar et al., 2019; Goswami et al., 2020）, and geothermal development（Li et al., 2020）. TEG technology has become a hot topic in recent years. The voltage and output power of a TEG chip are key indicators for evaluating TEG performance. Many studies on phase change materials（Selvam et al., 2020）, combustion mode （Rowe et al., 1998; Zhou et al., 2015）, Peltier Effect（Li et al., 2020; Wang et al., 2019）, and mechanical-electrical structures（Chen et al., 2017）were carried out to improve the thermoelectric power of TEG chips.

TEG chips are composed of many pairs (usually 127 legs) of thermocouples. The materials of thermocouples（Cheng et al., 2014; Karami et al., 2019; Siddique et al., 2019）, the geometry （Barry et al., 2016; Shittu et al., 2020; Chen et al., 2014）, interface layers（Xuan et al., 2002）, thermoelectric module（Cheng et al., 2014; Jia et al., 2019）, PN leg area and, the length of the n- and P-type thermoelectric legs affect the performance of TEG performance（Liu et al., 2018; Buchalik et al., 2019）. Many other scholars have analyzed the influence of the factors such as occupancy ratio（Rezania et al., 2014）, thermal conductivity（Rabari et al., 2015）, pressure（Du et al., 2014; Karthick et al., 2019）on the power of TEG.

Previous studies have mostly used multiple pairs of PN legs to test the performance of TEG chips. Some scholars have performed a numerical simulation of a pair of PN thermocouples. For example, （Schock et al., 2009）used Cobalt/Bi_2Te_3 based thermopile to make TEG for spacecraft, and its power generation chip contains 1-PN-TEG, with the power per unit area reaching about 0. 136 $W \cdot cm^{-2}$. （W. Wu , 2020）took a single pair of PN legs as the research object to analyze the power generation performance of Bi_2Te_3/Sb_2Te_3 alloy under low-temperature conditions in the case of constant and variable physical property.

The commonly used thermoelectric material for the low-temperature heat source (264 °C) is bismuth telluride (Bi_2Te_3-based) material. In general, the chip is made of 127 pairs of PN legs, copper electrode, ceramic (aluminum) plates. The conventional method to evaluate the chip performance is to directly test the output voltage and power of the whole TEG chip. However, the assembling of these PN legs to make a TEG chip for research is time-consuming. To save experimental time and TEG materials, we proposed an experimental method and developed the test apparatus for rapidly evaluating the performance of a whole TEG chip with 127 PN legs by using a TEG chip with

Contributed by the Advanced Energy Systems Division of ASME, this paper has
been published in the JOURNAL OF ENERGY RESOURCES TECHNOLOGY.

a single pair of PN legs. Using the experimental device developed in this study, we verified the feasibility of the proposed method with the experimental data from both 1-PN-TEG and 127-PN-TEG chips.

2. DESIGN OF TEG CHIP AND THE EXPERIMENTAL DEVICE

2.1 Experimental schematic

Fig. 1 is the schematic of the 1-PN-TEG chip used in this study. One side is the hot side (top side), and the other one is the cold side (bottom side). Heat is conducted from the hot to the cold side and converted into electric energy. A specific temperature gradient is generated between the two sides of the device. In a thermoelectric unit, the hot side electrons holes and holes electrons will move towards the cold side due to the temperature gradient field, resulting in a potential difference between the PN legs. If a digital load is connected to the circuit, an electric current flow through the circuit, and the direction of the current flows from the cold to hot side in the N legs and from the hot to the cold side in the P legs.

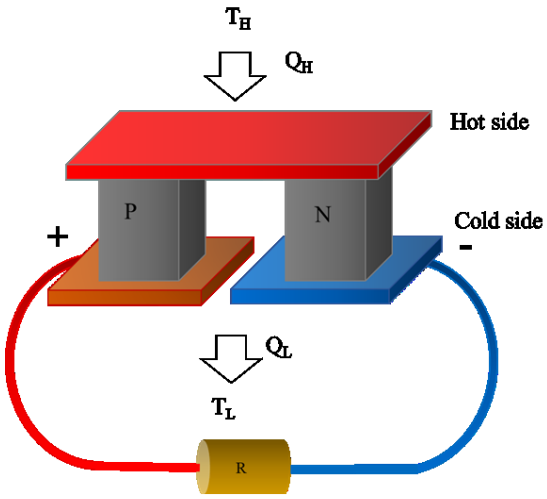

Figure 1: The schematic of 1-PN-TEG chip.

Because a single pair of PN legs can only generate a small electric potential, multiple PN legs are often connected in series to increase the electromotive force. In order to compare the voltage generated by the 1-PN-TEG chip with that by the 127-PN-TEG chip, a TEG chip with 127 PN legs was designed (Fig. 2a) and manufactured (Fig. 2b) in our laboratory. The TEG chip that we made for this study had the similar internal sandwich structure as that of the typical TEG on the market. The reason to make the 127-PN-TEG chips by ourselves, instead of buying from the market, was that the 1-PN-TEG chips are not available in the market. We had to manufacture the 1-PN-TEG chips. The property of the materials in the TEG chips from the market may not be the same as that of the materials used for the 1-PN-TEG chips. Therefore the 127-PN-TEG chips were manufactured in our laboratory in order to make sure that the materials (including thermoelectric, aluminum for top and bottom plates, and other materials) used in both the 1-PN-TEG and the 127-PN-TEG chips are the same. This provided the same basis to compare the two types of TEG chips. Note that the voltage generated by a 127-PN-TEG chip should be closely equal to 127 times of the voltage generated by a 1-PN-TEG chip.

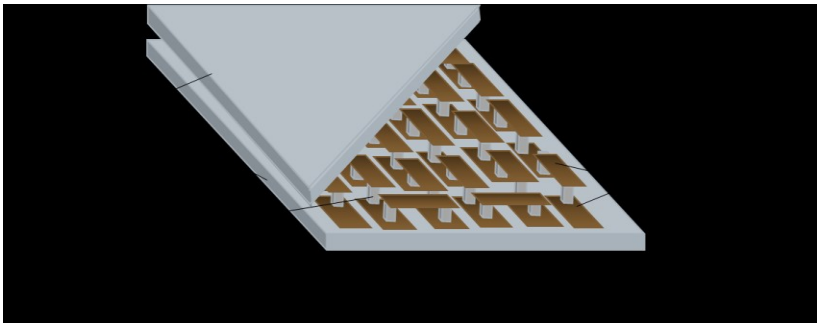

(a) Sectional view.

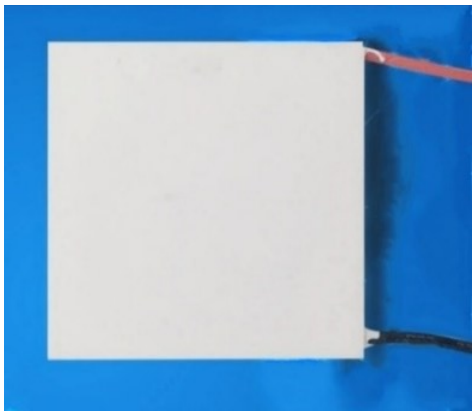

40×40 mm^2

(b) Picture of a 127-PN-TEG chip manufactured in this study.

Figure 2: Schematic diagram and the picture of a 127-PN-TEG chip.

2.2 Experimental process

A TEG test apparatus was designed in this study and the schematic is shown in Fig. 3. The lower side of the chip was connected to a heat source provided by the heating device, and the upper side was connected to a water-cooling system. The pressure was applied to make the water-cooling system, thermoelectric chip, and heat source in close contact. The open-circuit voltage of TEG chips could be recorded using a digital multimeter.

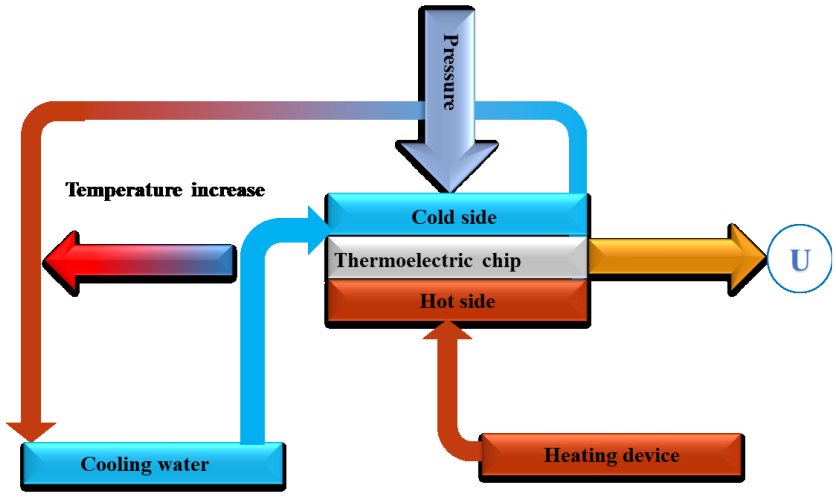

Figure 3: Process diagram of TEG test system.

3. BUILDING AND INSTALLATION OF EXPERIMENTAL APPARATUS

3.1 Construction of 1-PN-TEG

1-PN-TEG is the core part of the experimental unit, which consists of PN legs, copper plates, aluminum, and heat-conducting silicon grease. Four 1-PN-TEGs with different area (1-PN-TEG # 1: 1.4×1.4 mm^2, 1-PN-TEG # 2: 2.0×2.0 mm^2, 1-PN-TEG # 3: 2.6×2.6 mm^2, 1-PN-TEG # 4: 4.5×4.5 mm^2) are placed on the same aluminum substrate (Fig. 4). Due to the special thickness of 1-PN-TEG # 5, four 1-PN-TEG # 5 is on the same substrate. The chip fabrication procedures are as follows:

(a) A copper plate is placed on the aluminum, and the contact surface between the copper plate and the aluminum is coated with solder for fixation.

(b) Apply solder on the PN legs of different sections and place them on the copper plate, as shown in Fig. 5. Place another aluminum coated with a suitable amount of solder paste on it, fix it with a binder clip, and perform reflow soldering.

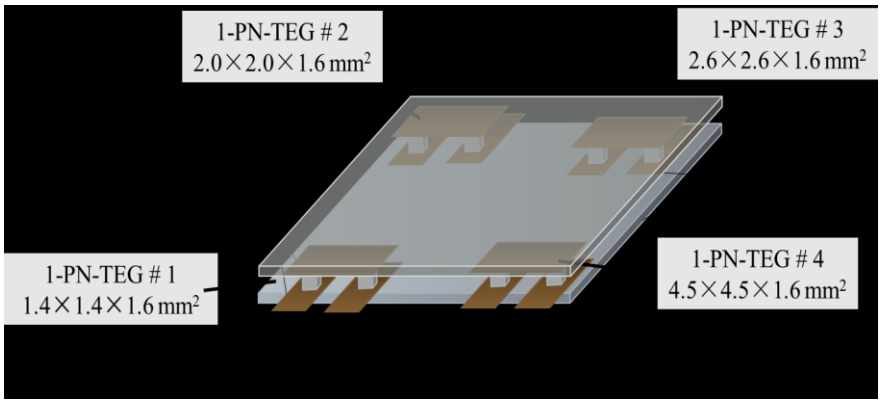

Figure 4: Schematic diagram of the 1-PN-TEGs structure.

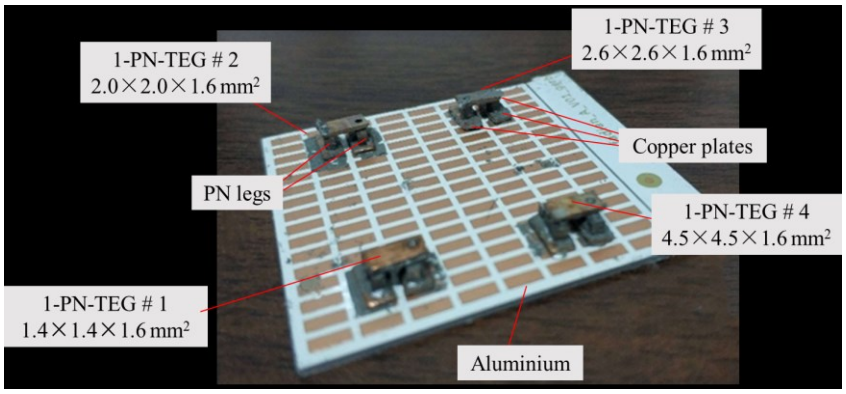

Figure 5: Photos of the four 1-PN-TEG chips.

3.2 Construction of the TEG test apparatus

We designed and built an experimental apparatus to measure the voltage of both 1-PN-TEG and 127-PN-TEG chips. The main parts, the basic arrangement and the photo of the TEG test system are shown in Fig. 6. The TEG test apparatus designed and constructed in this study was comprised of a heating device, TEG chips, water-cooling system, pressure sensor, and digital data acquisition tool. The effects of pressure and PN leg area on the performance of TEG have been investigated using the TEG test apparatus.

During the experiments, a heating device was used to simulate the heat source, with a temperature range of 0 - 450 °C and a control accuracy of ±0.1 °C, as shown in Fig. 6. The heating device's upper surface is smooth and flat. Thermally conductive silicone grease was used for a full and close contact, allowing a good heat transfer to the chips.

The pressure device (HANDPI 0992) is composed of a pressure sensor and a fixing frame, of which pressure range is 10 - 550 N. A cylindrical high-precision pressure sensor is placed on top of the water-cooled block, and the heating device is on the fixed frame. From the bottom to the top, the order is: fixed frame, heating device, TEG chip, water cooling block, pressure sensor (Fig. 6). The pressure was kept constant by adjusting the knob of the pressure gauge, so as to avoid the influence of pressure variation on the power and voltage of the chips.

The water-cooling system consists of a water-cooling block, a water tank, and a submersible pump. An aluminum water-cooling block is attached to the cold side of the TEG chips to serve as a heat sink. The inlet and outlet of the water-cooling block are connected to rubber pipes, as shown in Fig. 6. One end of the rubber pipe is linked to a miniature submersible pump in the water tank. Between the water-cooling block and the TEG chip, an appropriate amount of thermally conductive silicone grease is applied to reduce the contact thermal resistance and enhance the thermal conductivity. Besides, a high-precision miniature thermometer is used to measure the water temperature.

The electric circuit in the TEG test system consists of a data acquisition unit (Agilent 34972) and a digital load which could adjust the load to match the internal resistance of the TEG chips. The data acquisition unit was connected to the TEG's electrodes made of copper plates, and was used to measure the open-circuit voltage and output power of the TEG chips.

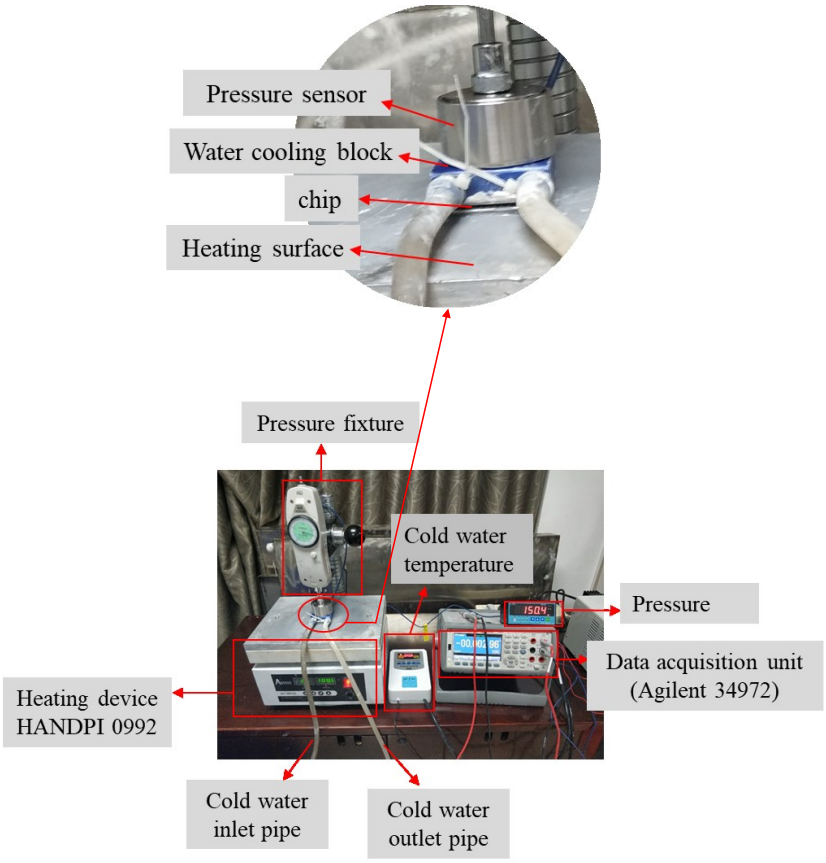

Figure 6: Basic structure and photo of the TEG test system.

4. RESULTS AND DISCUSSION

Five 1-PN-TEG chips with different parameters were fabricated in this study. The related parameters of each chip are shown in Table 1. The influence of the PN leg area and other factors on the open-circuit voltage of the 1-PN-TEG chips was analyzed. Occupation ratio is defined as the ratio of the PN leg area to the 1-PN-TEG area （Cheng et al., 2014）.

For all the experiments conducted in this study, the cold side temperature was set to 22 °C in each set, and the temperature difference between the hot and cold sides was controlled to rise from 25 to 100 °C. An appropriate amount of heat-conducting silicone grease is applied to the contact surface between the hot side or cold side and 1-PN-TEG chips to reduce the thermal resistance.

Table 1: Parameters of 1-PN-TEG chips.

1-PN-TEG number	1-PN-TEG #1	1-PN-TEG #2	1-PN-TEG # 3	1-PN-TEG # 4	1-PN-TEG # 5
PN leg size (mm^3)	1.4×1.4×1.6	2.0×2.0×1.6	2.6×2.6×1.6	4.5×4.5×1.6	1.4×1.4×1.9
Occupation ratio	0.0392	0.08	0.1352	0.405	0.0392

4.1 Effect of temperature difference on TEG performance

As shown in Fig. 7a, the experimental results demonstrate that the open-circuit voltage of 1-PN-TEG chips increases almost linearly with the temperature difference. This phenomenon observed in small size TEG chips with only one pair of PN legs is consistent with the experimental data measured in regular large size TEG chips with 127 pairs of PN legs（Li et al., 2020; Li et al., 2020; Cheng et al., 2014; Li et al., 2019; Liu et al., 2014; Rezania et al., 2013）. At a temperature difference of 70 °C, the corresponding open-circuit voltages of 1-PN-TEGs # 1, 2, 3, 4 are 0.02452, 0.0278, 0.0239, and 0.01765 V respectively. The open-circuit voltage of 1-PN-TEG # 4 increases the smallest.

The voltage per unit area increases monotonously with the temperature difference as shown in Fig. 7b. It can be seen that the voltage per unit leg area of 1-PN-TEG # 1 is the maximum. Note that 1-PN-TEG # 1 has the smallest PN leg area of PN legs. The effect of temperature difference on the voltage per unit leg area at different PN leg areas is more noticeable and more tendentious. The effect of PN leg area on the voltage will be discussed in next section in more details.

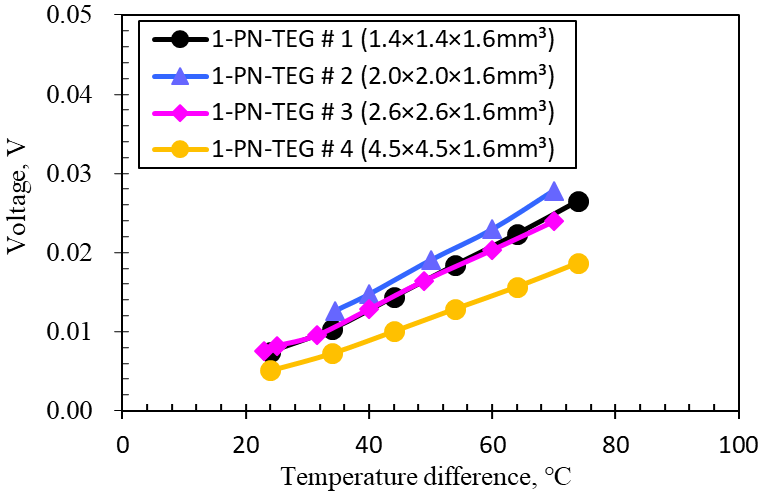

(a) The voltage of TEG chips vs. temperature difference.

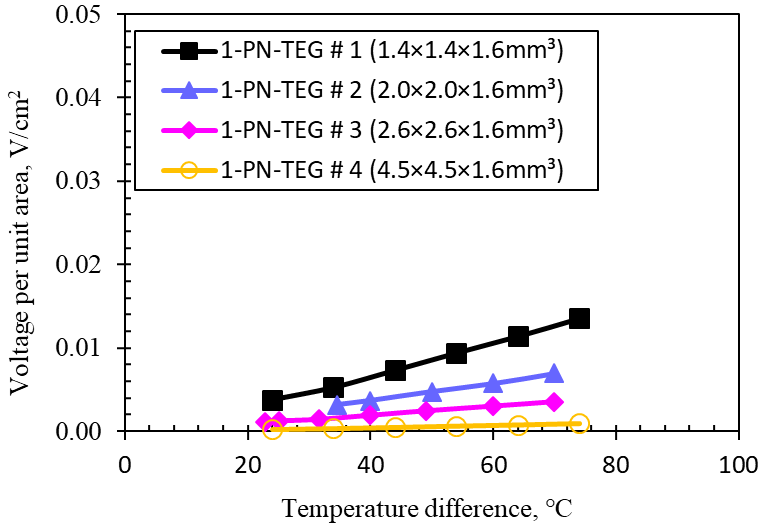

(b) The voltage per unit area of 1-PN-TEG chips vs. temperature difference.

Figure 7: The effect of temperature difference on the voltage per unit area of 1-PN-TEG chips at different PN leg areas.

According to Ohm's law of the closed circuit, the power of the TEG is given by:

$$P = IU_R = I^2R = \frac{E^2R}{(R+r)} = \frac{E^2}{\frac{(R-r)^2}{R} + 4r} \quad (1)$$

Where P is the power of TEG, r is the internal resistance of the TEG, E is the open-circuit voltage of the TEG, R is the external resistance, I is the load current, and UR is the voltage on the external resistance.

When $R = r$, $P = P_{max}$,

$$P_{max} = IU_R = I^2R = \frac{E^2R}{(R+r)} = \frac{E^2}{\frac{(R-r)^2}{R} + 4r} = \frac{E^2}{4r} \quad (2)$$

Here, P_{max} is the maximum power of a TEG.

We measured the voltage of four 1-PN-TEG chips with different PN leg areas at different temperatures. Then the values of power were calculated with Eq. 2 according to the experimental data.

Fig. 8a shows that the output power of 1-PN-tegchips with different PN leg areas increases with temperature difference. The output power per unit PN leg area of the 1-PN-TEG chips with temperature difference is shown in Fig. 8b. The tendency is similar to that shown in Fig. 7b.

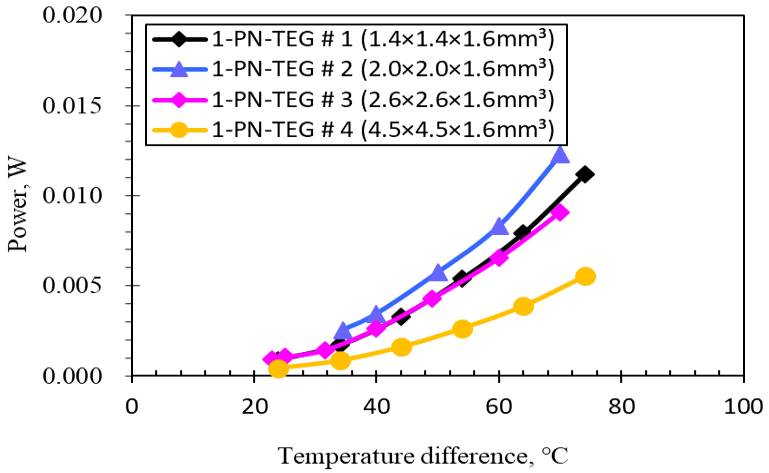

(a) The power of 1-PN-TEG chips vs. temperature difference at different PN leg areas.

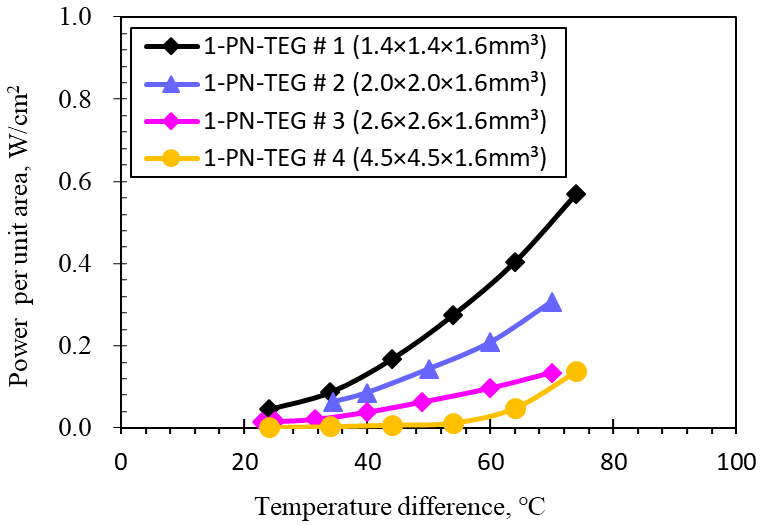

(b) The power per unit PN leg area of the 1-PN-TEGs vs. temperature difference.

Figure 8: The effect of temperature difference on the voltage per unit area of 1-PN-TEG chips at different PN leg areas.

4.2 Influence of PN leg area on TEG performance

The voltage of the 1-PN-TEG chips with different PN leg areas is shown in Fig. 9a. The effect of PN leg area on the voltage is not very clear. Fig. 9b shows the voltage per unit area of the 1-PN-TEG chips with different PN leg areas. The voltage per unit area of the 1-PN-TEG chips decreases rapidly with the increase in PN leg area.

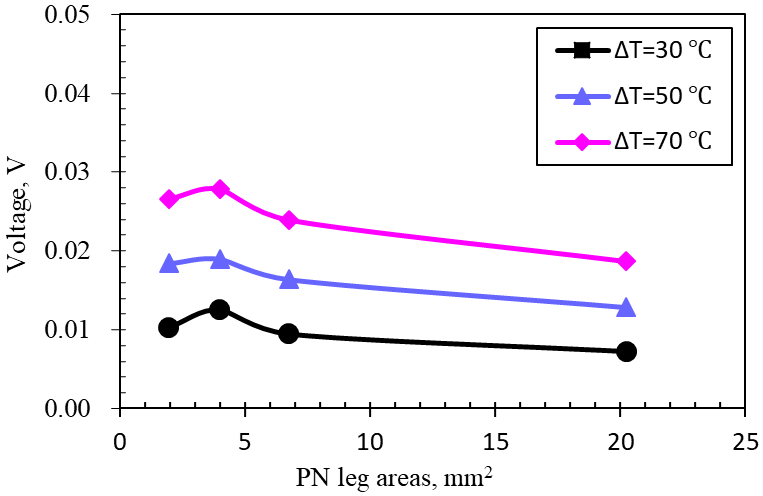

(a) Voltage of 1-PN-TEG chips vs. different PN leg area.

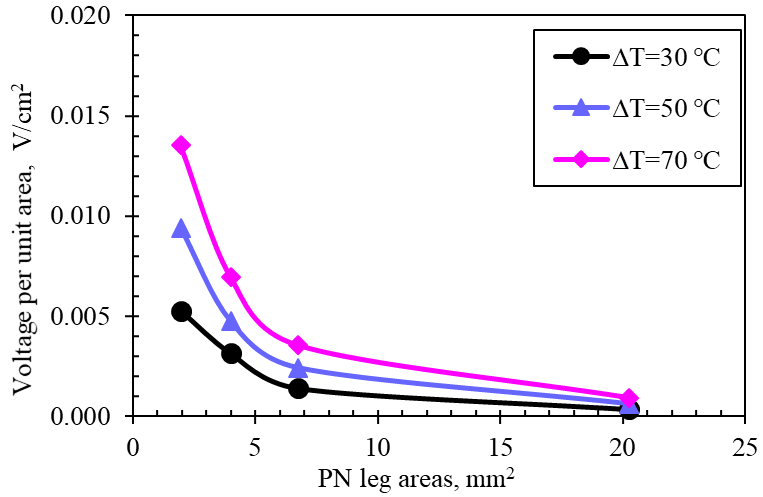

(b) Voltage per unit area of 1-PN-TEG chips vs. different PN leg area.

Figure 9: The effect of PN leg area on the voltage of the 1-PN-TEG chips (ΔT was equal to 30, 50, and 70 °C respectively)

Fig. 10a shows the effect of PN leg area on the output power of the 1-PN-TEG chips. It can be seen that the output power of the 1-PN-TEG chips increases first and then decreases as the PN leg area increases. The power output is maximized at a specific cross-sectional size, which is 4.0 mm^2 in this study. Fig 10b shows that the power per unit area of 1-PN-TEG chips decreases with the increases in PN leg area, which is consistent with the results reported previously（Wang et al., 2019; Du t al., 2014; Karthick et al., 2019; Freunek M. et al., 2009）.

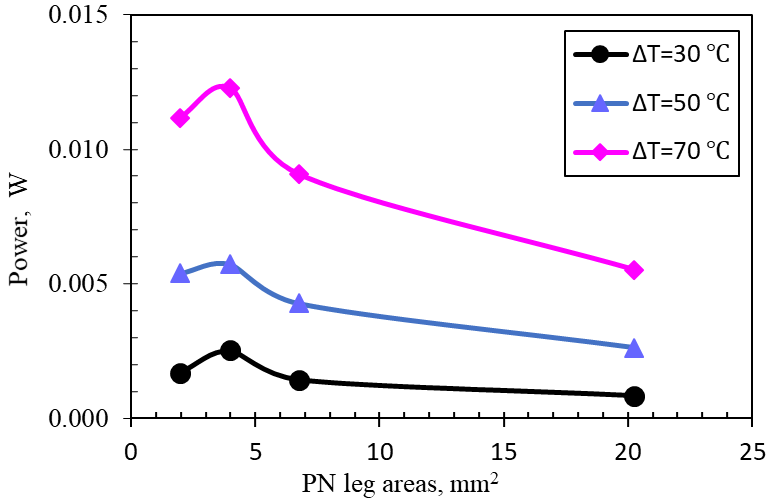

(a) The effect of PN leg area on the power of the 1-PN-TEG chips at different temperature differences.

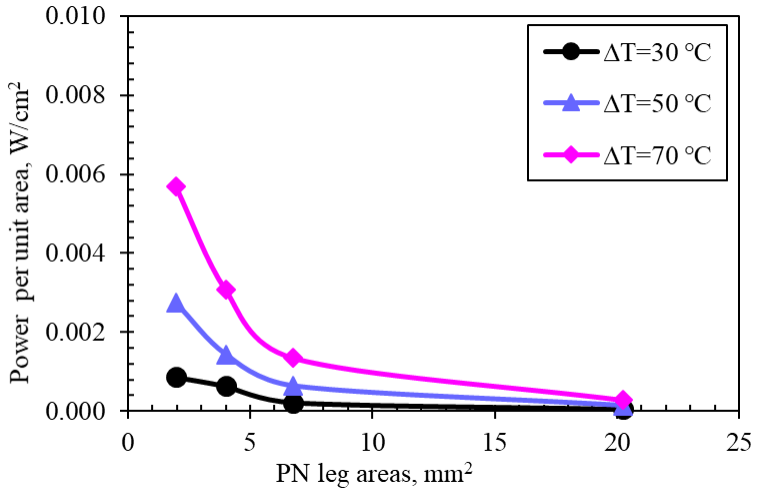

(b) The effect of PN leg area on the output power of the 1-PN-TEG chips per unit PN leg area.

Figure 10: The effect of PN leg area on the power of the 1-PN-TEG chips at different temperature differences.

4.3 Influence of occupation ratio on TEG performance

Fig 11a shows the effect of occupation ratio on the voltage of the 1-PN-TEG chips. It can be seen that the voltage of the 1-PN-TEG chips first increases and then decreases with the increase of occupation ratio. The effect of occupation ratio on the voltage per unit area of 1-PN-TEG chips is shown in Fig. 11b. The voltage per unit area decreases rapidly with the increase of occupation ratio.

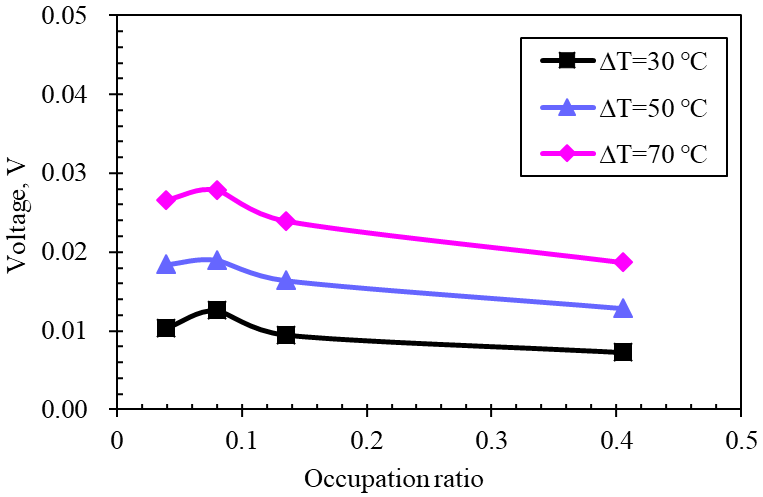

(a) The effect of occupation ratio on the voltage of 1-PN-TEG chips.

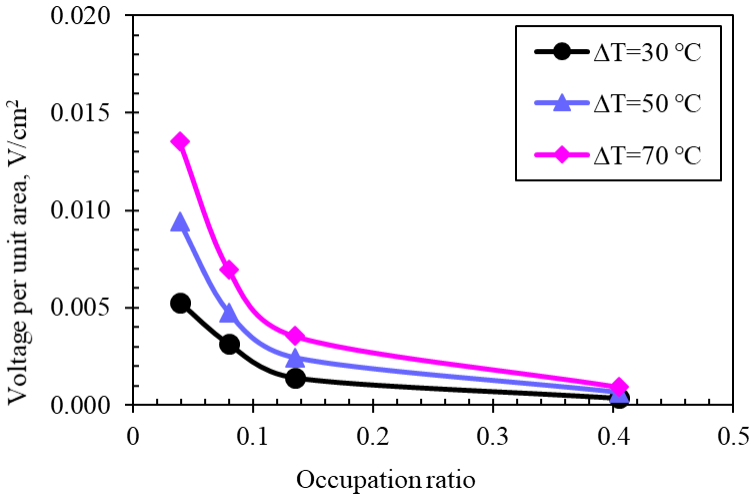

(b) The effect of occupation ratio on the voltage of 1-PN-TEG chips per unit area.

Figure 11: The effect of occupation ratio on the voltage of 1-PN-TEG chips at different temperature differences.

As shown in Fig. 12a, the power of 1-PN-TEG chips increases first and then decreases with the increase in occupation ratio. However, the power per unit area of 1-PN-TEG chips decreases with the increase in occupation ratio (see Fig. 12b). The experimental data from Cheng et al. （2016） were measured at a temperature difference of 60°C and are also depicted in Fig. 11b. One can see that the power of 1-PN-TEG chips obtained from this study is almost consistent with the results reported by Cheng et al. （2016）at the temperature differences.

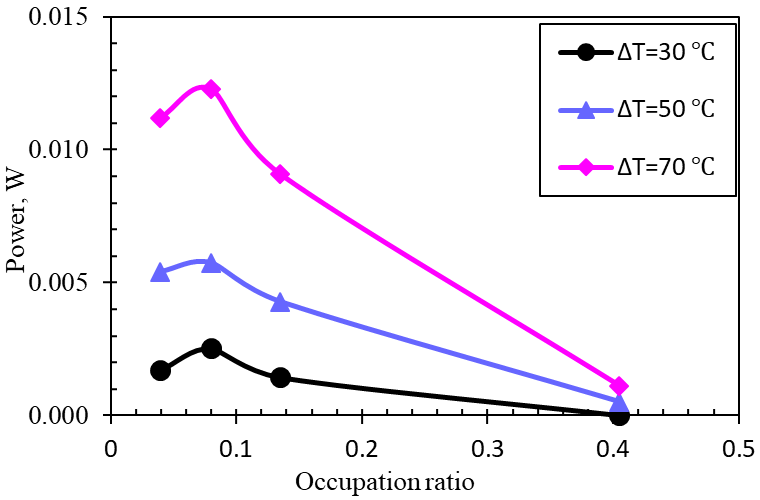

(a) The effect of occupation ratio on 1-PN-TEG chips output power.

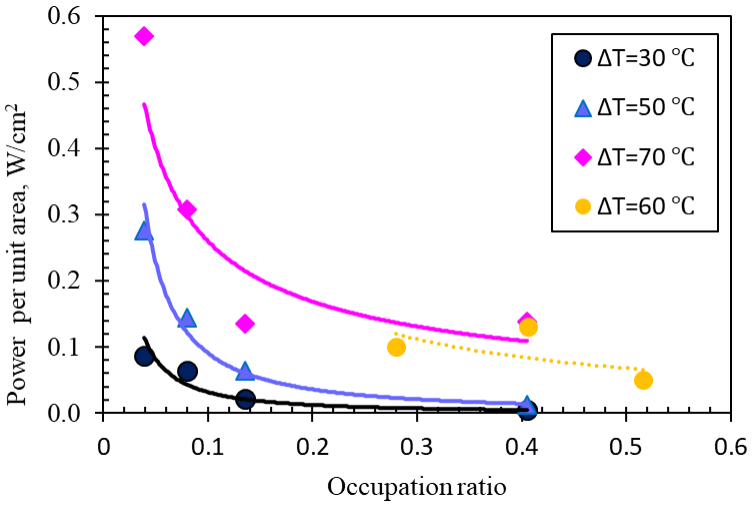

(b) The effect of occupation ratio on 1-PN-TEG chips Power per unit area.

Figure 12: The effect of occupation ratio on 1-PN-TEG chips Power at different temperature differences.

4.4 Influence of pressure on open-circuit voltage of the 1-PN-TEG chips

In this study, 1-PN-TEG # 5 was chosen to investigate the effect of pressure on the open-circuit voltage of the 1-PN-TEG chips. Two sets of pressures (120 and 160 N) were applied to evaluate the pressure effect.

The influence of pressure on the open circuit voltage at different temperature differences is shown in Fig. 13. The results show that the open-circuit voltage increases with the pressure applied to the chips. For example, the voltage was enhanced from 0.0169 to 0.01728 V when the pressure is increased from 120 to 160 N (ΔT = 45 °C).

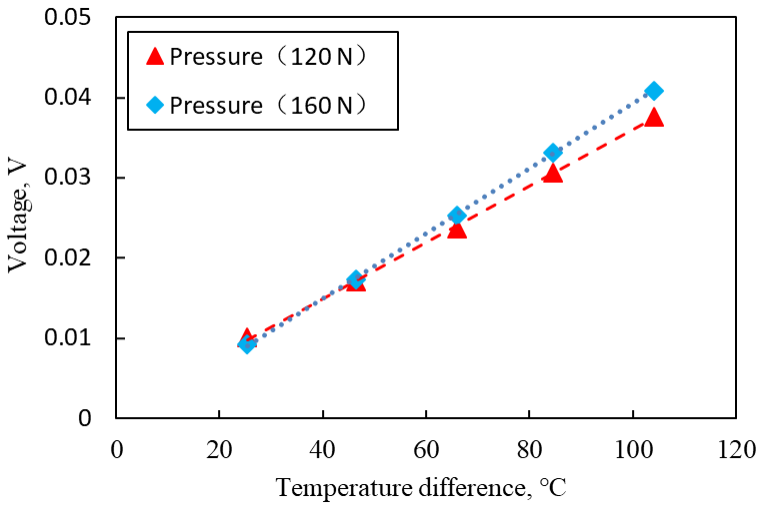

Figure 13: The influence of pressure on open-circuit voltage of the 1-PN-TEG # 5.

Fig. 14 shows the relationship between the pressure and the output power of 1-PN-TEG # 5. It can be seen that the output power of 1-PN-TEG # 5 also increases with the pressure and the temperature difference, which is consistent with the results reported by Du et al. The reason behind the above observation might be because that increasing the pressure could enhance the degree of contact between the 1-PN-TEG chips and heat sources.

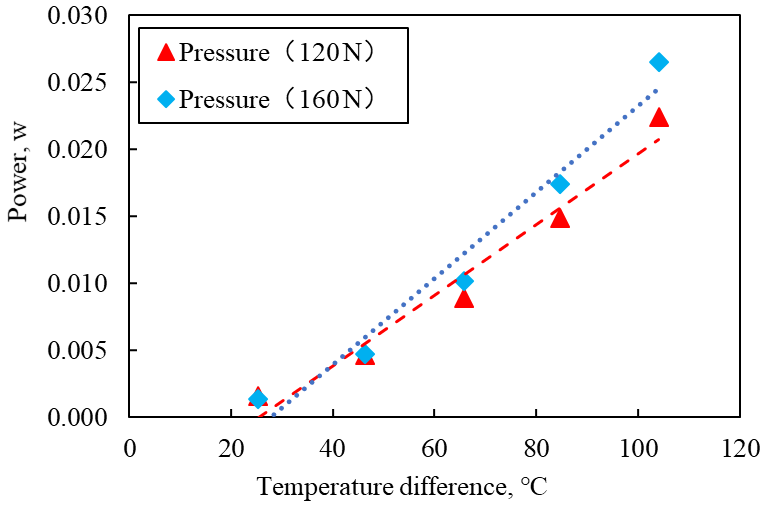

Figure 14: The influence of pressure on the output power of the 1-PN-TEG # 5.

4.5 Feasibility analysis through the voltage and power comparison between 1-PN-TEG and 127-PN-TEG chips.

The main purpose of this paper is to develop an experimental methodology and the apparatus to rapidly evaluate the performance of a whole TEG chip with 127 PN legs by using a simple TEG chip with only one pair of PN legs. The approach to verifying the feasibility of the proposed method is to compare the experimental data from both 1-PN-TEG and 127-PN-TEG chips. Theoretically the voltage or power generated by a 127-PN-TEG chip should be closely equal to 127 times of the voltage or power generated by a 1-PN-TEG chip. This is based on the assumption that the127 pairs of PN legs in the 127-PN-TEG chip are connected seriously. The feasibility of the proposed method will be analyzed and discussed in this section.

TEG chips with different size but the same material were made in our laboratory and were used for the feasibility verification. These chips are: 1-PN-TEG # 1 (1.4×1.4×1.6 mm^3), 1-PN-TEG # 5 (1.4×1.4×1.9 mm^3), 127-PN-TEG # 1 (1.4×1.4×1.6 mm^3), and 127-PN-TEG # 5 (1.4×1.4×1.9 mm^3). The voltage and power of 1-PN-TEG times 127 with 127-PN-TEG were measured by using the experimental

apparatus developed in this study. The results are demonstrated and compared in Fig. 15. During the experiments, the external pressure applied to the chips was 160 N. One can see that the voltage generated by a 127-PN-TEG chip was closely equal to 127 times of the voltage generated by a 1-PN-TEG chip. More specifically, the voltage of a 127-PN-TEG chip was a little less than 127 times of the voltage of a 1-PN-TEG chip, especially at higher temperature differences. This is actually reasonable because of the effect of the contact resistance on the voltage of the 127-PN-TEG chip.

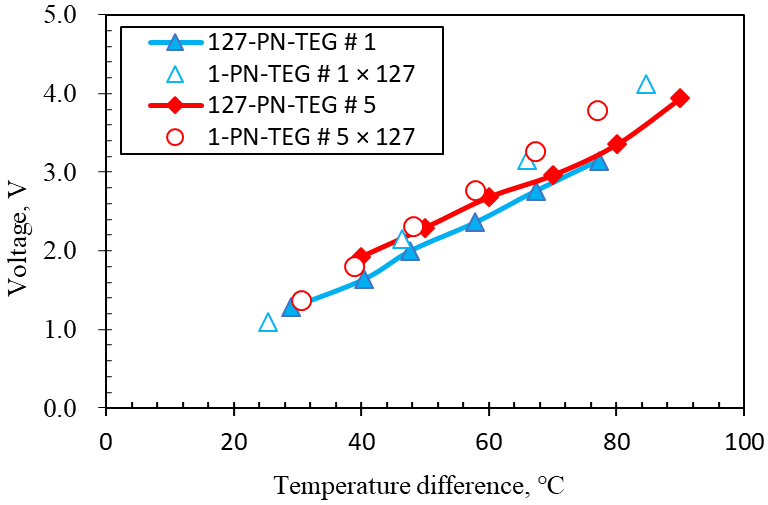

Figure 15: Comparison of the voltage of 1-PN-TEG (times 127) with that of 127-PN-TEGs.

The relationships between the power and the temperature difference in both 1-PN-TEG and 127-PN-TEG chips can be matched by the same type of mathematical model, i.e., quadratic equation (Fig.16).

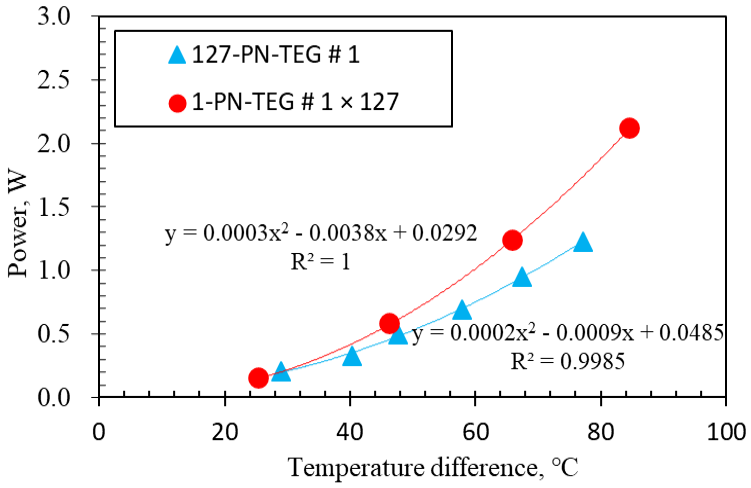

(a) 127-PN-TEG # 1 and 1-PN-TEG # 1 times 127.

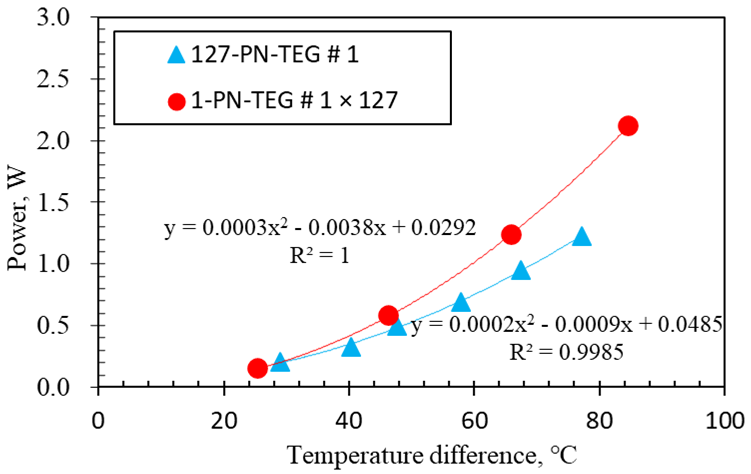

(b) 127-PN-TEG # 5 and 1-PN-TEG # 5 times 127.

Figure 16: Comparison of the output power of 1-PN-TEGs times 127 and 127-PN-TEGs.

5. CONCLUSIONS

This paper proposed an experimental method and developed a test apparatus to fast evaluate the performance of 127-PN-TEG by using the experimental data of 1-PN-TEG. At the same time, we also studied the influences of the temperature difference, the PN leg area, and the pressure on the output power of the TEG chips. The following conclusions may be obtained:

(1). The open-circuit voltage and the output power of the 127-PN-TEG chips measured experimentally were almost equal to those of the 1-PN-TEG chips by multiplying 127 at the same temperature differences.

(2). The open-circuit voltage and output power of 1-PN-TEG increased first and decreased as the PN leg area increases. The power output was maximized at a specific cross-sectional size, which was 2.0×2.0 mm^2 in this study.

(3). The open-circuit voltage and output power of 1-PN-TEG increased with the applied pressure when the temperature difference between the cold and hot sides of the 1-PN-TEG was kept constant.

(4). The open-circuit voltage and output power of 1-PN-TEG increased with the temperature difference between the cold and hot sides as well as the 127-PN-TEG.

(5). Using the test apparatus developed in this article, it is possible to evaluate the performance of a TEG chip with 127 PN legs by using the experimental data from a TEG chip with only one PN leg.

REFERENCES

Antonino, P., Daniele, B., Martin, C., David, V., Vladimir, K., Lukas, P., Silvia, C., Maurizio, S., and Marek, P., 2018, "Thermal Energy Harvesting on the Bodily Surfaces of Arms and Legs through a Wearable Thermo-Electric Generator," Sensors, 18(6), p. 1927.

Jaziri, N., Boughamoura, A., Mueller, J., Mezghani, B., and Ismail, M., 2019, "A Comprehensive Review of Thermoelectric Generators: Technologies and Common Applications," Energy.

Wang, X., Huang, Y., Cheng, C., Lin, D. T., and Kang, C., 2012, "A Three-Dimensional Numerical Modeling of Thermoelectric Device with Consideration of Coupling of Temperature Fi Eld and Electric Potential Fi Eld," Energy, 47(1), pp. 488–497.

Araiz, M., Casi, Á., Catalán, L., Martínez, Á., and Astrain, D., 2020, "Prospects of Waste-Heat Recovery from a Real Industry Using Thermoelectric Generators: Economic and Power Output Analysis," Energy Convers. Manag., 205(December 2019), p. 112376.

Crane, D. T., and Bell, L. E., 2009, "Design to Maximize Performance of a Thermoelectric Power Generator With a Dynamic Thermal Power Source," J. Energy Resour. Technol., 131(1).

Al-Nimr, M. A., Tashtoush, B., and Hasan, A., 2020, "A Novel Hybrid Solar Ejector Cooling System with Thermoelectric Generators," Energy, 198(May1), pp. 117318.1-117318.17.

Li, K., Bian, H., Liu, C., Zhang, D., and Yang, Y., 2015, "Comparison of Geothermal with Solar and Wind Power Generation Systems," Renew. Sustain. Energy Rev., 42, pp. 1464–1474.

Shittu, S., Li, G., Akhlaghi, Y. G., Ma, X., Zhao, X., and Ayodele, E., 2019, "Advancements in Thermoelectric Generators for Enhanced Hybrid Photovoltaic System Performance," Renew. Sustain. Energy Rev., 109(JUL.), pp. 24–54.

Venkateshwar, K., Siddique, A. R. M., Tasnim, S., Simha, H., and Mahmud, S., 2020, "Thermoelectric Generator Integrated Solar Air Heater: A Compact Passive System," J. Energy Resour. Technol., pp. 1–36.

Goswami, R., and Das, R., 2020, "Experimental Analysis of a Novel Solar Pond Driven Thermoelectric Energy System," J. Energy Resour. Technol., 142(12).

Li, K., Garrison, G., Moore, M., Zhu, Y., Liu, C., Hepper, J., Bandt, L., and Petty, S., 2020, Field Test of Thermoelectric Generators at Bottle Rock Geothermal Power Plant.

Selvam, C., Manikandan, S., Krishna, N. V., Lamba, R., and Mahian, O., 2020, "Enhanced Thermal Performance of a Thermoelectric Generator with Phase Change Materials," Int. Commun. Heat Mass Transf., 114, p. 104561.

Rowe, D. M., and Gao Min, 1998, "Evaluation of Thermoelectric Modules for Power Generation," J. Power Sources, 73(2), pp. 193–198.

Zhou, S., Sammakia, B. G., White, B., Borgesen, P., and Chen, C., 2015, "Multiscale Modeling of Thermoelectric Generators for Conversion Performance Enhancement," Int. J. Heat Mass Transf., 81(feb.), pp. 639–645.

Li, K., Garrison, G., Moore, M., Zhu, Y., Liu, C., Horne, R., and Petty, S., 2020, "An Expandable Thermoelectric Power Generator and the Experimental Studies on Power Output," Int. J. Heat Mass Transf., 160.

Wang, J., Cao, P., Li, X., Song, X., Zhao, C., and Zhu, L., 2019, "Experimental Study on the Influence of Peltier Effect on the Output Performance of Thermoelectric Generator and Deviation of Maximum Power Point," Energy Convers. Manag., 200(June), p. 112074.

Chen, J., Li, K., Liu, C., Li, M., Lv, Y., Jia, L., and Jiang, S., 2017, "Enhanced Efficiency of Thermoelectric Generator by Optimizing Mechanical and Electrical Structures," Energies, 10(9), pp. 1329-.

Cheng, F., Hong, Y., and Zhu, C., 2014, "A Physical Model for Thermoelectric Generators With and Without Thomson Heat," J. Energy Resour. Technol., 136(1), p. 11201.

Karami Rad, M., Rezania, A., Omid, M., Rajabipour, A., and Rosendahl, L., 2019, "Study on Material Properties Effect for Maximization of Thermoelectric Power Generation," Renew. Energy, 138, pp. 236–242.

Siddique, A. R. M., Kratz, F., Mahmud, S., and Van Heyst, B., 2019, "Energy Conversion by Nanomaterial Based Trapezoidal-Shaped Leg of Thermoelectric Generator (TEG) Considering Convection Heat Transfer Effect," J. Energy Resour. Technol., 141(8), pp. 082001.1-082001.11.

Barry, M. M., Agbim, K. A., Rao, P., Clifford, C. E., Reddy, B. V. K., and Chyu, M. K., 2016, "Geometric Optimization of Thermoelectric Elements for Maximum Efficiency and Power Output," Energy, 112, pp. 388–407.

Shittu, S., Li, G., Zhao, X., and Ma, X., 2020, "Review of Thermoelectric Geometry and Structure Optimization for Performance Enhancement," Appl. Energy, 268.

Chen, W. H., Wang, C. C., and Hung, C. I., 2014, "Geometric Effect on Cooling Power and Performance of an Integrated Thermoelectric Generation-Cooling System," Energy Convers. Manag., 87, pp. 566–575.

Xuan, X. C., Ng, K. C., Yap, C., and Chua, H. T., 2002, "A General Model for Studying Effects of Interface Layers on Thermoelectric Devices Performance," Int. J. Heat Mass Transf., 45(26), pp. 5159–5170.

Cheng, F., Hong, Y., and Chao, Z., 2014, "Structure Optimization of a BiTe-Based Thermoelectric Module," High Volt. Technol., 40(005), pp. 1599–1604.

Jia, X., and Guo, Q., 2020, "Design Study of Bismuth-Telluride-Based Thermoelectric Generators Based on Thermoelectric and Mechanical Performance," Energy, 190, p. 116226.

Liu, T., and Yang, Z., 2018, "Performance Assessment and Optimization of a Thermophotovoltaic Converter–Thermoelectric Generator Combined System," J. Energy Resour. Technol., 140(7).

Buchalik, R., Nowak, I., Rogozinski, K., and Nowak, G., 2019, "Detailed Model of a Thermoelectric Generator Performance," J. Energy Resour. Technol., 142(2).

Rezania, A., Rosendahl, L. A., and Yin, H., 2014, "Parametric Optimization of Thermoelectric Elements Footprint for Maximum Power Generation," J. Power Sources, 255, pp. 151–156.

Rabari, R., Mahmud, S., and Dutta, A., 2015, "Effect of Thermal Conductivity on Performance of Thermoelectric Systems Based on Effective Medium Theory," Int. J. Heat Mass Transf., 91(DEC.), pp. 190–204.

Du, Q., Zhang, Y., and Yu, S., 2014, "Influence of Contact Pressure on the Performance of Thermoelectric Generator," J. Tianjin Univ. (Natural Sci. Eng. Technol. Ed., 47(01), pp. 9–14.

Karthick, K., Suresh, S., Singh, H., Joy, G. C., and Dhanuskodi, R., 2019, "Theoretical and Experimental Evaluation of Thermal Interface Materials and Other Influencing Parameters for Thermoelectric Generator System," Renew. Energy, 134, pp. 25–43.

Schock, H., Caillet, T., Case, E., Fleurial, J. P., Hogan, T., Lyle, M., Maloney, R., Moran, K., Ruckle, T., Sakamoto, J., Sheridan, T., Shih, T., Thompson, T., Timm, E., Zhang, L., and Zhu, G., 2010, "Thermoelectric Conversion of Waste Heat to Electricity in an IC Engine Powered Vehicle," Glob. Powertrain Congr. 2010, GPC 2010 TROY - Proc., 59, pp. 258–283.

WU, W., MA, C., CHEN, Y., and DOU, Y., 2020, "Numerical Simulation and Simulation of Low Temperature Semiconductor Thermoelectric Power Generation Unit," Power Technol., 44(1), pp. 85–89.

Li, K., Garrison, G., Moore, M., Zhu, Y., Liu, C., Horne, R., and Petty, S., 2019, "Experimental Study on the Effects of Flow Rate and Temperature on Thermoelectric Power Generation," Proceedings, pp. 1–10.

Liu, C., Chen, P., and Li, K., 2014, "A 500 W Low-Temperature Thermoelectric Generator: Design and Experimental Study," Int. J. Hydrogen Energy.

Rezania, A., Yazawa, K., Rosendahl, L. A., and Shakouri, A., 2013, "Co-Optimized Design of Microchannel Heat Exchangers and Thermoelectric Generators," Int. J. Therm. Sci., 72, pp. 73–81.

Freunek, M., Müller, M., Ungan, T., Walker, W., and Reindl, L. M., 2009, "New Physical Model for Thermoelectric Generators," J. Electron. Mater., 38(7), pp. 1214–1220.

Cheng, F., Hong, Y., Zhang, B., and Tang, W., 2016, "Experimental Optimization of the Area-Specific Power for Thermoelectric Modules," Spacerfaft Envoriment Engeering, 33(4).